MOLECULAR AND CELLULAR BIOLOGY, Nov. 1994, p. 7385–7393
0270-7306/94/$04.00+0

Vol. 14, No. 11

cis-Regulatory Sequences Responsible for Alternative Splicing of the *Drosophila dopa decarboxylase* Gene

JIE SHEN AND JAY HIRSH*

Biology Department, University of Virginia, Charlottesville, Virginia 22903

Received 13 June 1994/Returned for modification 13 July 1994/Accepted 17 August 1994

The *Drosophila dopa decarboxylase* gene, *Ddc*, is expressed in the hypoderm and in specific sets of cells in the central nervous system (CNS). The unique *Ddc* primary transcript is alternatively spliced in these two tissues. The *Ddc* CNS mRNA contains all four exons (A through D), whereas the hypodermal mRNA contains only three exons (A, C, and D). To localize *cis*-regulatory sequences responsible for *Ddc* alternative splicing, a *Ddc* minigene and several fusion genes containing various amounts of *Ddc* sequences fused to *fushi tarazu* (*ftz*) exon 1 were constructed and introduced into flies by P-element-mediated germ line transformation. We find that *Ddc* intron ab and exon B are sufficient to regulate *Ddc* alternative splicing, since transcripts of a minimal fusion gene containing most of *Ddc* intron ab and exon B are spliced to exon B in the CNS but not in the hypoderm. These results indicate that *Ddc* alternative splicing is regulated by either a negative mechanism preventing splicing to exon B in the hypoderm or a positive mechanism activating splicing to exon B in the CNS. Our previous data suggest that *Ddc* hypodermal splicing is the actively regulated splicing pathway (J. Shen, C. J. Beall, and J. Hirsh, Mol. Cell. Biol. 13:4549–4555, 1993). Here we show that deletion of *Ddc* intron ab sequences selectively disrupts hypodermal splicing specificity. These results support a model in which *Ddc* alternative splicing is negatively regulated by a blockage mechanism preventing splicing to exon B in the hypoderm.

Alternative splicing provides an important mechanism to regulate gene expression in eukaryotes (12, 22, 24, 28). A single pre-mRNA can be alternatively spliced to generate multiple mRNAs which encode functionally distinct proteins. Regulation of alternative splicing often occurs in a tissue-specific and/or developmental stage-specific fashion.

Most insights into regulatory mechanisms of alternative splicing have been obtained from studies of *Drosophila melanogaster*. Alternative splicing can be controlled via negatively or positively acting regulatory mechanisms. Examples of negatively regulated splicing are the female-specific splicing of *Sex lethal* (*Sxl*) and *transformer* (*tra*) primary transcripts, as well as the repression of somatic splicing of P-element transposase pre-mRNAs. *Sxl* regulates the alternative splicing of its own pre-mRNAs (2, 3) and *tra* pre-mRNAs (35). In females, the *Sxl* protein prevents the use of the *Sxl* male-specific exon and the *tra* non-sex-specific exon. Multiple *cis*-acting elements, both upstream and downstream of the *Sxl* male exon, are required for this autoregulation (14, 15). The mechanism by which *Sxl* regulates alternative splicing of *tra* is better understood. The *Sxl* protein inhibits splicing to the non-sex-specific exon by binding specifically to the polypyrimidine tract, blocking the binding of the essential splicing factor, U2AF (41). The alternative splicing of the P-element transposase pre-mRNA is regulated by preventing the splicing of the third intron in somatic cells, which is spliced in germ cells. This somatic repression is achieved by inhibiting binding of U1 small nuclear ribonucleoprotein to the accurate 5′ splice site (33, 34). Two pseudo-5′ splice sites in the 5′ exon are required for this negative regulation (21, 34). Regulation of the female-specific *double sex* (*dsx*) splicing is the only example of positive splicing regulation reported for *D. melanogaster* (30). The polypyrimidine tract of the *dsx* female-specific 3′ splice site is interrupted by purines (9). Protein products of *tra* and *transformer-2* (*tra-2*) activate this nonconsensus 3′ splice site in females by recruiting general splicing factors to the enhancer elements located downstream of the female 3′ splice site (9, 13, 39, 40).

Many genes in both vertebrates and *D. melanogaster* are alternatively spliced in neural versus nonneural tissues. Examples include the vertebrate genes encoding c-Src (23, 27), calcitonin/CGRP (29), and N-CAM (31) and the *Drosophila* genes *Ultrabithorax* (*Ubx*) (20), *antennapedia* (*Antp*) (37), *neuroglian* (16) and *dopa decarboxylase* (*Ddc*) (25). Potential *cis* elements responsible for regulating this alternative splicing have been identified for the genes encoding c-Src (5, 6), calcitonin/CGRP (11), and N-CAM (38) but not for any of these *Drosophila* genes.

We use *Ddc* as a model system to study the regulatory mechanism of the neural versus nonneural alternative splicing in *D. melanogaster*. The *Ddc* primary transcript is expressed primarily in the central nervous system (CNS) and the hypoderm (25), where *Ddc* is alternatively spliced into different mRNAs encoding distinct DDC isoforms. The *Ddc* CNS-specific mRNA contains four exons (A through D), whereas the hypodermal mRNA contains only three (A, C, and D), skipping the second exon. In the CNS, *Ddc* is expressed only in about 150 dopamine and serotonin neurons and in a subset of glial cells (1, 19). In the hypoderm, *Ddc* is expressed in most if not all hypodermal cells (8). *Ddc* CNS-specific splicing is regulated in a tissue-specific rather than cell-specific manner, as shown by splicing patterns following overexpression of the *Ddc* primary transcript in all cells in flies (32).

The hypodermal splicing of *Ddc* is selectively affected by heat shock (32). During heat shock, the CNS-specific splice form accumulates inappropriately in the hypoderm, whereas *Ddc* splicing in the CNS is unaffected. This result suggests that *Ddc* hypodermal splicing is the regulated pathway, whereas the CNS splicing pathway is the default. In this report, we show that partial deletion of the *cis* sequences regulating *Ddc* alternative splicing leads to accumulation of the CNS splice form in the hypoderm. These results reinforce our previous

* Corresponding author. Phone: (804) 982-5608. Fax: (804) 982-5626. Electronic mail address (Internet): jh6u@virginia.edu.

TABLE 1. Oligonucleotide primers

Primer	Sequence	Description[a]
For PCR analyses		
Ddc exon A	5′GCTCTAGAGTTAAGAGGAGAACGCCAAGCG	
Ddc exon B	5′ATCCGGCGAAATGTTAGCTTTACC	
Ddc exon D	5′GAGCTCCACTCAGCATGTCCGCAAC	
Hsp70	5′GAGCTCAAACAAGCGCAGCGAACAAGC	
Bluescript polylinker	5′GCAGGAATTCGATATCAAGCTTATCG	
For plasmid construction		
167	5′GCCCATGGGTATACGAGCTGCTGCACTAATAAGC	*Ddc* intron AB 745 to 764, starting with synthetic *Nco*I and *Xca*I sites
168	5′CGCCATGGGTATACTTTAGTTATCAGACGTGCAT	*Ddc* intron BC 1040 to 1021, starting with synthetic *Nco*I and *Xca*I sites
169	5′CGCCATGGAGATCTAAGTCGACCATTGTCTTGGC	*Ddc* exon C 1114 to 1095, starting with synthetic *Nco*I and *Bgl*II sites
217	5′CGGAATTCTGCGTGACTCAAAAGG	*Gapdh-2* −578 to −557
218	5′GGGGTACCGAGCTCGCACAATTTTGTTGACGGAAGTTG	*Gapdh-2* 29 to 6, starting with synthetic *Kpn*I and *Sac*I sites
228	5′CGCGAATTCTAGGCCTTTCTGGCGGACAAC	*Hsp70* −369 to −349, starting with a synthetic *Eco*RI site
229	5′GCGGGTACCGAGCTCATTGTTTAGCTTGTTCGCTGCGC	*Hsp70* +79 to +57, starting with synthetic *Kpn*I and *Sac*I sites

[a] Positions are numbered from the start site of transcription.

model that the *Ddc* hypodermal splicing pathway is actively regulated. The regulated hypodermal splicing of *Ddc* could be a result of either blockage of the exon B 3′ splice site or activation of the exon C 3′ splice site, such that it is used preferentially to the exon B 3′ splice site. To distinguish between these two models, we constructed two fusion genes in which *Ddc* exon B and various amounts of intron ab are fused to *fushi tarazu* (*ftz*) exon 1. We find that the fusion gene containing *Ddc* exon B and most of intron ab is sufficient to prevent splicing to exon B in the hypoderm. These results demonstrate that the *cis*-regulatory sequences responsible for *Ddc* alternative splicing are located within intron ab and exon B.

MATERIALS AND METHODS

Oligonucleotides. Oligonucleotide primers (Table 1) were synthesized on a Milligen Cyclone Plus synthesizer and used without purification following deprotection.

Plasmid construction. Plasmid JS#13 (*Hsp70/DdcABC*) contains the *Hsp70* promoter region and part of its transcription unit (−369 to +79), joined to genomic *Ddc* sequences spanning from the *Ssp*I site within exon A (+72) to the *Sal*I site within exon C (+1107), joined to the distal portion of *Ddc* exon D (+3601 to +3830) containing the polyadenylation signal. The DNA segment containing the *Hsp70* promoter region was generated by PCR using primers 228 and 229, *Drosophila* genomic DNA as a template, and *Taq* DNA polymerase. The PCR product was digested with *Eco*RI and *Sac*I (*Hsp70/Eco*RI-*Sac*I). The *Ddc*ABC fragment was generated from an intermediate plasmid, JS#3. JS#3 was obtained by inserting the genomic *Ddc Ssp*I-*Sal*I segment (exon A [+72] to exon C [+1107]) into the *Sma*I and *Sal*I sites of Bluescript KS. JS#3 was cut with *Sac*I and *Sal*I (*Ddc*ABC/*Sac*I-*Sal*I). The DNA segment containing *Ddc* polyadenylation region was also obtained from an intermediate plasmid, JS#7. The genomic *Ddc Nsi*I-*Spe*I fragment (exon D +3601 to +3830) was blunted with T4 DNA polymerase and Klenow DNA polymerase and cloned into the *Sma*I site of Bluescript KS and Bluescript SK to generate JS#7 KS and JS#7 SK, respectively. JS#7 KS was cut with *Sal*I and *Not*I (*Ddc*D/*Sal*I-*Not*I). These three DNA fragments (*Hsp70/Eco*RI-*Sac*I, *Ddc*ABC/*Sac*I-*Sal*I, and *Ddc*D/*Sal*I-*Not*I) were ligated and cloned into the *Not*I and *Eco*RI sites of the P-element transformation vector CaSpeR 3 (26) to generate *Hsp70/DdcABC*.

Plasmid JS#22 [*Hsp70/ftz1.DdcBC*(l)] contains the same segments of the *Hsp70* promoter region and the distal portion of *Ddc* exon D as JS#13, but the *Ddc* sequence +72 to +301 was substituted with the genomic *ftz* segment from the *Sal*I site within exon 1 to the *Xca*I site within the *ftz* intron. JS#15 [*Hsp70/ftz1.DdcBC*(s)] is essentially the same as JS#22 except that it lacks *Ddc* intron ab +301 to +745. JS#20 [*Hsp70/ftz1.DdcB*(l)] is the same as JS#22 except that it lacks *Ddc* sequence from +969 within exon B to +1107 within exon C. JS#16 [*Hsp70/ftz1.DdcB*(s)] is essentially the same as JS#15 except that it lacks *Ddc* +969 to +1107. These constructs were made via a series of intermediate plasmids as following. The *Ddc* segment containing *Ddc* from intron ab (+745) to exon C (+1114) was generated by PCR using primers 167 and 169, *Ddc* plasmid DNA as a template and Vent DNA polymerase. The PCR product was digested with *Xca*I and *Bgl*II and inserted into the *Xca*I (within the *ftz* intron) and *Bgl*II (within the *ftz* exon 2) sites of a *ftz*-Bluescript plasmid (a gift from Jamila Horabin) to generate JS#2. The PCR generated region of JS#2 was confirmed by sequencing. The *Sal*I fragment of JS#2, from *ftz* exon 1 to *Ddc* exon C, was cloned into the *Sal*I site of Bluescript SK to generate JS#6. The *Ddc* segment containing *Ddc* from intron ab (+745) to intron bc (+1140) was generated by PCR using primers 167 and 168, *Ddc* plasmid DNA as a template, and Vent DNA polymerase. The PCR product was digested with *Xca*I and inserted into the *Xca*I site within the *ftz* intron of the same *ftz*-Bluescript plasmid to generate JS#1. The PCR generated region of JS#1 was also confirmed by sequencing. The *Sal*I-*Sac*I fragment of JS#1, from *ftz* exon 1 to *ftz* exon 2, was inserted into the *Sal*I and *Sac*I sites of Bluescript SK to yield JS#5. The DNA segment containing the *Gapdh-2* promoter region (−578 to +29) was generated by PCR using primers 217 and 218, *Gapdh-2* plasmid DNA (D937; a gift from John Lis's laboratory) as a template, and Vent DNA polymerase. The *Eco*RI-*Kpn*I fragment of this PCR product containing the *Gapdh-2* promoter region, together with the *Kpn*I-*Sac*I fragment of JS#5 and the

*Sac*I-*Pst*I fragment of JS#7 SK, was cloned into the *Pst*I and *Eco*RI sites of the CaSpeR 2 vector to generate JS#9. JS#14 was made similarly except that the *Eco*RI-*Kpn*I fragment of the *Gapdh-2* PCR product for JS#9 was substituted with the *Eco*RI-*Kpn*I fragment of the *Hsp70* PCR product which was also used for constructing JS#13. JS#11 was made by ligating the smaller *Kpn*I-*Xba*I fragment (0.7 kb) of JS#6 with the larger *Kpn*I-*Xba*I fragment (8.6 kb) of JS#9.

JS#15 [*Hsp70/ftz1.DdcBC*(s)] was generated by inserting the *Kpn*I-*Hpa*I fragment (0.9 kb) of JS#11 into the *Kpn*I and *Hpa*I sites of JS#14. JS#16 [*Hsp70/ftz1.DdcB*(s)] was made by self-ligating the larger *Bam*I fragment (9.1 kb) of JS#14. The *Xca*I-*Sty*I fragment (0.7 kb) of JS#3 was inserted into the *Xca*I and *Sty*I sites of JS#6 to generate JS#19-X. JS#20 [*Hsp70/ftz1.DdcB*(l)] was then made by inserting the *Kpn*I-*Bam*I fragment (1.0 kb) of JS#19-X into the *Kpn*I and *Bam*I sites of JS#16. The *Kpn*I-*Xba*I fragment (1.2 kb) of JS#19-X was inserted into the *Kpn*I and *Xba*I sites of JS#11 to generate an intermediate construct, JS#21. JS#22 [*Hsp70/ftz1.DdcBC*(l)] was then made by inserting the *Kpn*I-*Hpa*I fragment (1.4 kb) of JS#21 into the *Kpn*I and *Hpa*I sites of #15.

Sequences of *ftz*, *Hsp70*, and *Gapdh-2* were obtained from GenBank and are numbered from the start of transcription. All of the JS# constructs were used for P-element germ line-mediated transformation and contain w^+ as a marker. These constructs were injected into *yw* embryos with a helper plasmid which encodes transposase but is incapable of transposition itself (18).

RT-linked PCR (RT-PCR). All tissues were hand dissected from late-third-instar larvae under a dissecting microscope on an ice-chilled block. Larvae were heat shocked at 38°C for 1 h as described previously (32). The amount of tissue used per reverse transcription (RT) reaction was CNS from 20 larvae or hypoderm from 5 larvae. Tissues were allowed to dissolve at 4°C for 0.5 to 24 h in 0.5 ml of solution D (4 M guanidinium thiocyanate [Fluka], 25 mM sodium citrate [pH 7], 0.5% sarcosyl, 0.1 M 2-mercaptoethanol) (10). Then, 0.05 ml of 2 M sodium acetate (pH 4), 0.5 ml of phenol (water saturated), and 0.1 ml of chloroform-isoamyl alcohol mixture (49:1) were added sequentially to the homogenate. The mixture was mixed thoroughly by vortexing and cooled on ice for 15 min. Samples were microcentrifuged for 15 min at 4°C, and then 0.4 ml of the aqueous phase was transferred to a fresh tube and mixed with 0.1 ml of phenol (water saturated) and 0.1 ml of chloroform-isoamyl alcohol mixture (49:1). The phases were separated by microcentrifugation for 15 min at room temperature. To ensure that the RNA preparations were free of genomic DNA contamination, only 0.2 ml of the aqueous phase was transferred to a fresh tube; RNA was precipitated by mixing with 2.5 μl of 20-mg/ml glycogen (Boehringer Mannheim Biochemicals) and 0.6 ml of ethanol and then placed at −70°C for at least 30 min. After RNA was recovered by microcentrifugation at 4°C, the RNA pellet was washed vigorously twice with 70% ethanol and then resuspended in 10 μl of 10 mM Tris-HCl (pH 7.5)–1 mM EDTA.

Conditions for RT and PCR were the same as described previously (32) except that thermal cycling was performed with the following program: 94°C for 1 min, 65°C for 1 min, and 72°C for 1 min for 40 cycles (for detection of basal-level transcripts) or 35 cycles (for detection of heat shock-induced transcripts), followed by incubation at 72°C for 7 min. The identities of PCR products were confirmed by sequencing or reamplification of PCR products, using intronic and exonic primer pairs. We find little integration site-specific variation between transformant lines; when detected, these are noted in the text. Positive and negative controls were routinely performed to check for the integrity of the RNA preparations, function of the RT-PCR, and the presence of contaminating DNA. Primers specific for either the Bluescript polylinker or *Ddc* exon B were used to prime RT of RNAs from *Hsp70/DdcABC*, *Hsp70/ftz1.DdcBC*(l), and *Hsp70/ftz1.DdcBC*(s) or *Hsp70/ftz1.DdcB*(l) and *Hsp70/ftz1.DdcB*(s), respectively. The *Hsp70* transcription unit-specific primer was then used as a second primer during PCR to specifically amplify fusion cDNAs. As a positive control, endogenous *Ddc* transcripts were amplified by using the *Ddc* exon D-specific primer for RT and primers specific for exons A and D for PCR. Results of the positive controls are omitted except for *Hsp70/DdcABC* strain 1 shown in Fig. 2. Controls for contaminating genomic DNA in RNA preparations were done by using an aliquot of RT products and primers specific for the *Hsp70* promoter and transcription unit (Fig. 1) to PCR amplify nontranscribed *Hsp70* and fusion DNAs. The results of the negative controls for *Hsp70/ftz1.DdcB*(l) and *Hsp70/ftz1.DdcB*(s) are shown in Fig. 4.

RESULTS

A *Ddc* minigene containing 1.1 kb of *Ddc* from exons A to C is sufficient for the regulation of *Ddc* alternative splicing. To determine whether the exons and introns involved in *Ddc* alternative splicing are sufficient for its regulation, we constructed *Hsp70/DdcABC*, a *Ddc* minigene expressed under the control of a *Drosophila Hsp70* heat shock promoter. *Hsp70/DdcABC* contains 1.1 kb of *Ddc* sequences from the *Ssp*I site within exon A to the *Sal*I site in exon C, fused to the distal portion of *Ddc* exon D containing the polyadenylation signal (Fig. 1). This fusion gene was introduced into flies by P-element-mediated germ line transformation.

To distinguish *Hsp70/DdcABC* RNAs from endogenous *Ddc* RNAs, we used RT-PCR. As shown in Fig. 1, primers specific for the Bluescript polylinker and *Ddc* exon D were used to prime RT of *Hsp70/DdcABC* RNAs and endogenous *Ddc* RNAs, respectively. Primers specific for the *Hsp70* transcription unit and the Bluescript polylinker were then used to amplify cDNAs from *Hsp70/DdcABC* RNAs, or primers specific for *Ddc* exon A and exon D were used to amplify endogenous *Ddc* transcripts.

In the absence of heat shock, *Hsp70/DdcABC* is spliced predominantly into the CNS form in the CNS (Fig. 2, lanes 1 and 3) and the hypodermal form in the hypoderm (Fig. 2, lanes 2 and 4). Multiple independent strains containing *Hsp70/DdcABC* at different chromosomal locations were analyzed and gave similar though not identical results. Results from two strains are shown in Fig. 2. Strain 1 shows nearly absolute tissue specificity (Fig. 2, lanes 1 and 2). In contrast, strain 20 consistently accumulates a small amount of the CNS splice form in the hypoderm, as well as a small amount of an aberrant splice form (labeled * in Fig. 2, lane 4). These minor differences between strains could be due to differences in specific expression patterns caused by enhancers near insertion sites. The splicing patterns of endogenous *Ddc* transcripts show nearly absolute tissue specificity (Fig. 2, lanes 5 and 6).

Heat shock affects *Ddc* alternative splicing, causing accumulation of the CNS splice form in the hypoderm (32). During severe heat shock, the CNS-specific splice form is the predominant spliced product in the hypoderm from the heat shock-induced *Hsp70/Ddc* transgene. We find that the splicing of *Hsp70/DdcABC* transcripts responds similarly to heat shock. After 1 h of heat shock at 38°C, the CNS-specific splice form is the major spliced product in the hypoderm (Fig. 2, lanes 2′ and 4′). The CNS-specific splicing pathway is largely unaffected by

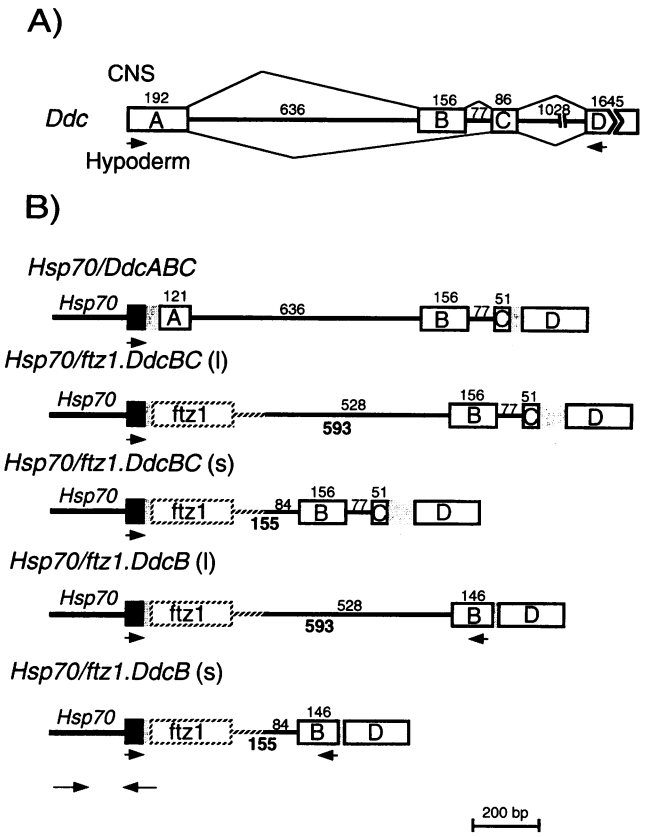

FIG. 1. (A) Alternative splicing of *Ddc* in the CNS and in the hypoderm. (B) Structure of a *Ddc* minigene and *ftz-Ddc* fusion genes. All constructs are drawn to scale except *Ddc* intron cd and exon D. *Ddc* exons are shown as open boxes labeled A, B, C, and D, and *ftz* exon 1 is shown as cross-hatched boxes labeled ftz1. Shaded gray or black boxes are Bluescript polylinkers or *Hsp70* transcription units, respectively. Solid lines are *Ddc* introns, and dashed lines are *ftz* introns. Numbers above boxes and lines indicate the lengths of *Ddc* exons and introns, whereas those below indicate the total lengths of fusion introns. All five fusion constructs contain the *Hsp70* promoter and 79 bp of its transcription unit, as well as 229 bp of the distal portion of *Ddc* exon D containing the polyadenylation signal. Arrows indicate the 5′→3′ orientation of primers. The shorter arrows indicate the locations of primers used for RT-PCR analysis of transcripts, whereas the longer arrows indicate the locations of primers used for PCR amplification of genomic DNA.

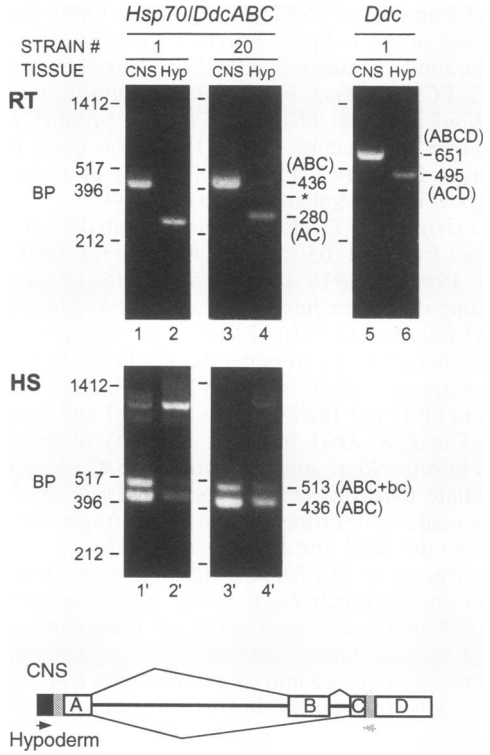

FIG. 2. *Hsp70/DdcABC* transcripts show normal regulation of *Ddc* alternative splicing. Total RNA was isolated from late-third-instar larval CNS and hypoderm (Hyp). *Hsp70/DdcABC* and endogenous *Ddc* transcripts were converted into cDNAs by RT using primers complementary to the Bluescript polylinker and the *Ddc* exon D (indicated as short arrows in Fig. 1 and 2). Primers specific for the *Hsp70* transcription unit or *Ddc* exon A were then used as a second primer during PCR to amplify *Hsp70/DdcABC* or endogenous *Ddc* cDNA, respectively. Strains 1 and 20 are two independent transformant lines in which *Hsp70/DdcABC* is inserted at different chromosomal locations. The 436-bp band (ABC) represents the CNS-specific splice form from *Hsp70/DdcABC* containing all three exons (lanes 1 and 3), whereas the 280-bp band (AC) is the hypodermal splice form (lanes 2 and 4). The 651-bp band (ABCD) represents the CNS splice form from endogenous *Ddc*, whereas the 495-bp band (ACD) is the hypodermal splice form. The molecular weight of the band labeled * suggests that this species results from use of a cryptic 3′ splice site within exon B. Use of this cryptic 3′ splice site has been observed previously in another context, in which case the identity of the splice product was confirmed by sequencing (unpublished results). During heat shock (HS), the CNS splice form (ABC) and the intron bc-containing splicing intermediate (ABC+bc) are the predominant spliced products in both tissues. In the original photographs, the hypodermal splice form (AC) band is present as an extremely faint band in lanes 2′ and 4′; these bands did not survive photographic processing. The identity of the intron bc containing species was confirmed by PCR reamplification using exonic and intron bc primer pairs. The high-molecular-weight bands are of lengths consistent with their identification as amplification products of precursor RNAs containing both intron ab and intron bc. Although severe heat shock does not block *Ddc* splicing in larvae, splicing of *Ddc* introns ab and bc is slowed in heat shock-induced *Hsp70/Ddc* genes (32).

heat shock, except that an intron bc-containing splicing intermediate accumulates in both tissues (Fig. 2, lanes 1′ to 4′), as has been seen for *Hsp70/Ddc* (32). We conclude that *Hsp70/DdcABC* contains all of the *cis*-regulatory sequences required for the regulation of *Ddc* alternative splicing.

The *Ddc* exon A 5′ splice site is not required for the regulation of *Ddc* alternative splicing. *Ddc* alternative splicing involves a common exon A 5′ splice site and two alternative 3′ splice sites of exons B and C. To test whether the regulation of *Ddc* alternative splicing requires the common 5′ splice site, we constructed *Hsp70/ftz1.DdcBC*(I), a fusion gene in which *Ddc* exon A 5′ splice site is substituted with the 5′ splice site of the *Drosophila ftz* gene (Fig. 1). *Hsp70/ftz1.DdcBC*(I) is essentially the same as *Hsp70/DdcABC*, except that *Ddc* exon A and the 5′ portion of the flanking intron ab are substituted with the 3′ portion of *ftz* exon 1 and its flanking intron. The *ftz* 5′ splice site was chosen because it conforms well to the 5′ splice site consensus sequence and is spliced efficiently in vivo (14) and in vitro (34).

In the absence of heat shock, normal splicing specificity of *Hsp70/ftz1.DdcBC*(I) transcripts is maintained in both tissues. The CNS-specific splice form (1BC) is found in the CNS (Fig. 3, lane 1), whereas the hypoderm-specific splice form (1C) is

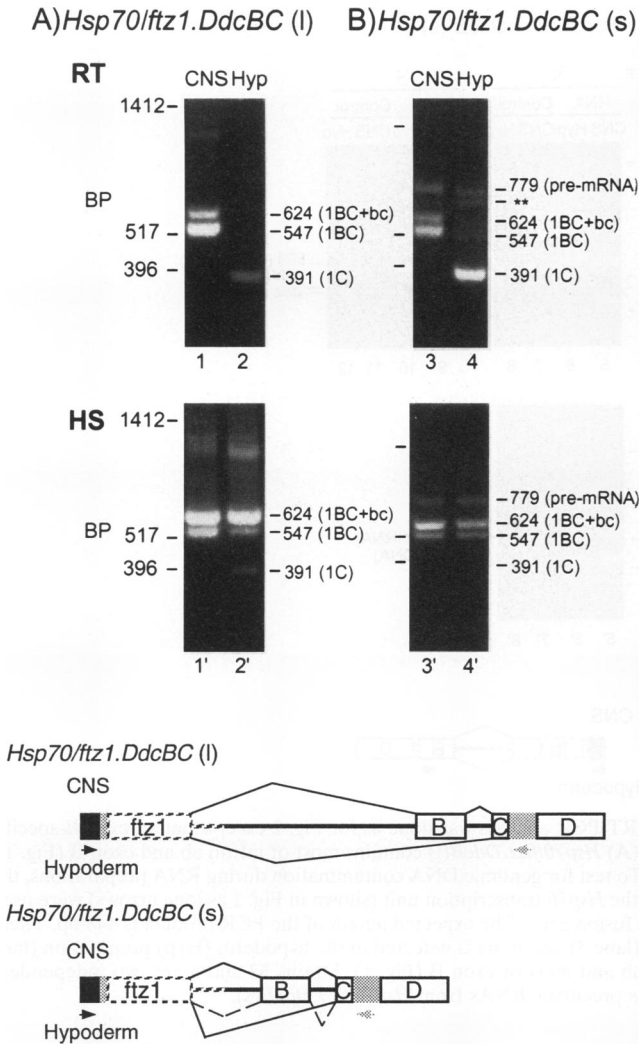

FIG. 3. Alternative splicing of *Hsp70/ftz1.DdcBC* fusion genes. RT-PCR analyses were carried out as for Fig. 2. Solid lines joining the boxes indicate major splicing events, whereas dashed lines represent minor splicing events. (A) *Hsp70/ftz1.DdcBC*(l) contains 528 bp of intron ab (Fig. 1). The band labeled 1C represents the hypodermal (Hyp) splice form, and the band labeled 1BC represents the CNS form. The splicing intermediate (1BC+bc) for the CNS-specific splicing accumulates in the CNS at room temperature and in both tissues during heat shock (HS). (B) *Hsp70/ftz1.DdcBC*(s) contains only 84 bp of intron ab, which includes the putative branch point site (Fig. 1). The CNS-specific splice form (1BC) and splicing intermediates (1BC+bc) are found in the hypoderm. The molecular weight of the band labeled ** suggests that this species is the intron 1b-containing splicing intermediate. The CNS splice form and its splicing intermediates are present in the hypoderm of three independent transformant lines tested (unpublished data). The 779-bp band is from precursor RNA, since the negative control for genomic DNA yields no amplification under the same PCR conditions (data not shown). In the original photograph, the hypodermal splice form (1C) is present as a very faint band in lane 4'; this band did not survive photographic processing. The identity of the intron bc-containing species was confirmed as described in the legend to Fig. 2.

the only splice product found in the hypoderm (Fig. 3, lane 2). In the CNS, more intron bc-containing splicing intermediates (1BC+bc) are observed from *Hsp70/ftz1.DdcBC*(l) (Fig. 3, lane 1) than from *Hsp70/DdcABC* (Fig. 2, lane 1). The splicing specificity of *Hsp70/ftz1.DdcBC*(l) is affected by heat shock similarly to that of *Hsp70/DdcABC* except that higher levels of intron bc-containing splicing intermediates are found from *Hsp70/ftz1.DdcBC*(l) (Fig. 3, lanes 1' and 2') than from *Hsp70/DdcABC* (Fig. 2, lanes 1' to 4') in both tissues. The increased detection of intron bc-containing intermediates relative to the *Hsp70/DdcABC* gene could be explained by the possibility that the *ftz1/DdcB* intron splices more rapidly than the *Ddc* ab intron. This is a likely possibility, since the *ftz* 5' splice site conforms to the consensus sequence better than the *Ddc* 5' splice site. These results demonstrate that the substituted 5' splice site of *Ddc* exon A is not necessary for the regulation of *Ddc* alternative splicing and that the remaining portion of *Ddc* in *Hsp70/ftz1.DdcBC*(l) is sufficient for this regulation.

To test whether all of the remaining 528 bp of intron ab in *Hsp70/ftz1.DdcBC*(l) is required for the regulation of *Ddc* alternative splicing, we constructed *Hsp70/ftz1.DdcBC*(s), which retains only 84 bp of intron ab, including the putative branch point site, but is otherwise identical to *Hsp70/ftz1.DdcBC*(l) (Fig. 1). The splicing of *Hsp70/ftz1.DdcBC*(s) is normal in the CNS (Fig. 3, lane 3), but the splicing specificity is reduced in the hypoderm (Fig. 3, lane 4). Although the hypodermal splice form (1C) is the major spliced product, the CNS splice form (1BC) and the splicing intermediate (1BC+bc) are also found in the hypoderm. During heat shock, the CNS splice form accumulates inappropriately in the hypoderm (Fig. 3, lanes 3' and 4'), as has been seen for *Hsp70/ftz1.DdcBC*(l) (Fig. 3, lanes 1' and 2'). These results indicate that intron ab sequences between 84 and 528 bases upstream of exon B contain partial *cis*-regulatory elements required for absolute tissue specificity of *Ddc* splicing in the hypoderm. Alternatively, the length of the intact 636-base intron might be the critical determinant for the regulated hypodermal splicing, although we know of no precedent in which reducing intron size alone at this size range disrupts regulated splicing specificity. The reduced hypodermal splicing specificity in *Hsp70/ftz1.DdcBC*(s) strongly supports our previous model that *Ddc* hypodermal splicing is the regulated splicing pathway (32).

***Ddc* intron ab and exon B are sufficient to block splicing to exon B in the hypoderm.** *Ddc* alternative splicing is achieved by skipping exon B in the hypoderm. Two models could explain this regulated hypodermal splicing. First, a blockage mechanism could prevent the use of the exon B 3' splice site. Alternatively, a positive regulatory mechanism could activate the exon C 3' splice site, such that it is used preferentially to the exon B 3' splice site in the hypoderm. Here we distinguish between these models by analyzing a fusion gene, *Hsp70/ftz1.DdcB*(l), in which the 3' portion of *ftz* exon 1 and flanking intron are fused to *Ddc* intron ab and exon B, in the absence of *Ddc* intron bc and exon C (Fig. 1).

The spliced product of *Hsp70/ftz1.DdcB*(l) accumulates in the CNS (Fig. 4, lane 1), whereas the unspliced pre-mRNA accumulates in the hypoderm (Fig. 4, lane 2). This result demonstrates that the *Ddc* sequences in this fusion gene are sufficient to prevent splicing to the exon B 3' splice site in the hypoderm and that competition from the exon C 3' splice site is not required for this regulation. Thus, we rule out the model in which *Ddc* alternative splicing is regulated by a positive mechanism activating the 3' splice site of exon C in the hypoderm. In these experiments, it is essential to completely remove genomic DNA from the RNA preparations, since the band labeled as the unspliced pre-mRNA could be derived from amplification of genomic DNA. Controls for genomic DNA contamination were done by PCR amplifying an aliquot of the RT product with primers specific for the nontranscribed *Hsp70* and *Hsp70/ftz1.DdcB*(l) DNA (Fig. 4, lanes 3 and 4).

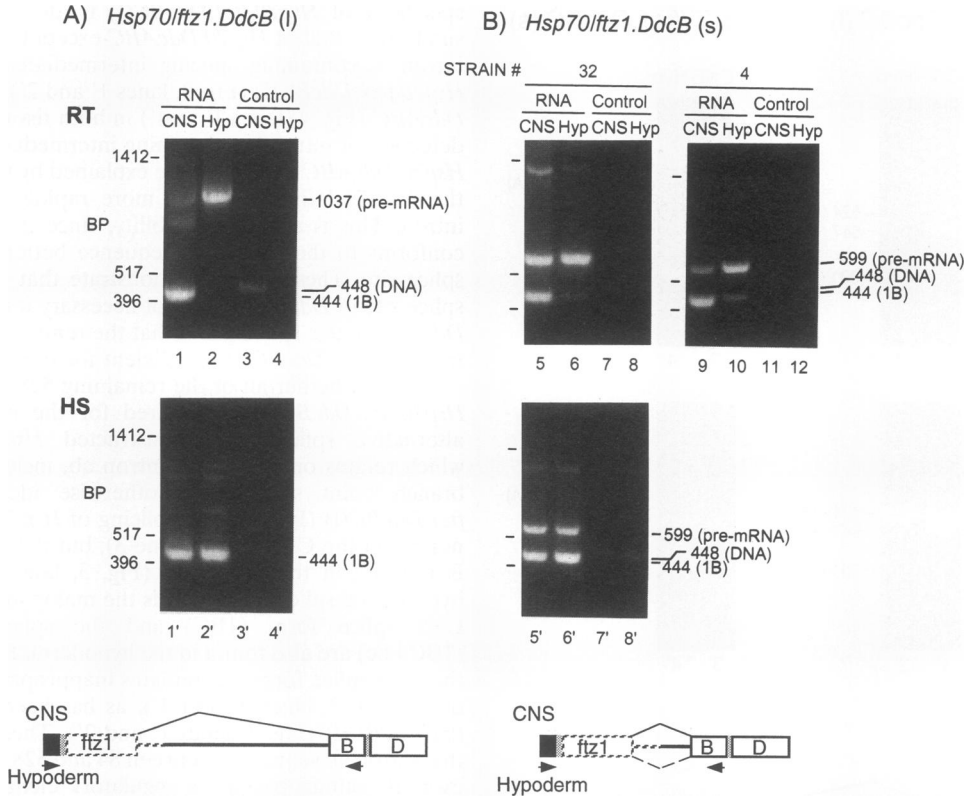

FIG. 4. *Hsp70/ftz1.DdcB* genes show tissue-specific alternative splicing. RT-PCR analysis was done as for Fig. 2 except that an exon B-specific primer was used for RT and later as the 3′ primer for PCR (Fig. 1 and 4). (A) *Hsp70/ftz1.DdcB*(l) contains most of intron ab and exon B (Fig. 1). The band labeled 1B represents the spliced product of *Hsp70/ftz1.DdcB*(l). To test for genomic DNA contamination during RNA preparations, the same RT products and primers specific for the *Hsp70* promoter region and the *Hsp70* transcription unit (shown in Fig. 1 as long arrows) were used during PCR to amplify genomic DNA of *Hsp70* and the *Hsp70/ftz1.DdcB*(l) fusion gene. The expected length of the PCR product is 448 bp. There is a small amount of contaminating genomic DNA in the CNS preparation (lane 3), but none is detected in the hypoderm (Hyp) preparation (lane 4). HS, heat shock. (B) *Hsp70/ftz1.DdcB*(s) contains the 3′ end of intron ab and most of exon B (Fig. 1). Strains 32 and 4 are two independent transformant lines containing the fusion gene. The 599-bp band represents precursor RNAs from *Hsp70/ftz1.DdcB*(s).

The 1,037-bp band is from the unspliced precursor RNA (Fig. 4, lane 2), since PCR with primers specific for genomic DNA yields no amplification product (Fig. 4, lane 4).

During heat shock, splicing of *Hsp70/ftz1.DdcB*(l) is no longer inhibited in the hypoderm, such that the spliced RNA accumulates in both tissues (Fig. 4, lanes 1′ and 2′). This result indicates that heat shock relieves inhibition of *Hsp70/ftz1.DdcB*(l) splicing in the hypoderm, such that splicing to exon B occurs in the hypoderm during heat shock. This alteration in tissue specific splicing is analogous to the effects seen with all previous *Ddc* constructs.

To further localize the *cis*-regulatory sequences for *Ddc* alternative splicing, we constructed *Hsp70/ftz1.DdcB*(s), which contains a 230-bp segment of *Ddc* consisting of 84 bp of intron ab and 146 bp of exon B (Fig. 1). The pre-mRNA of this fusion gene is consistently spliced more efficiently in the CNS (Fig. 4, lanes 5 and 9) than in the hypoderm (Fig. 4, lanes 6 and 10), as shown for two independent strains. These results show that this 230-bp segment of *Ddc* contains important regulatory sequences required to inhibit splicing to the exon B 3′ splice site in the hypoderm. In comparison with *Hsp70/ftz1.DdcB*(l), the degree of splicing blockage in the hypoderm is reduced, and splicing is slowed even in the CNS. These results indicate that the regulatory sequences located within intron ab between 84 to 528 bases upstream of exon B are required for complete blockage of splicing to exon B in the hypoderm and for efficient general splicing. As for *Hsp70/ftz1.DdcB*(l), heat shock also relieves the hypodermal blockage of *Hsp70/ftz1.DdcB*(s) splicing, such that the splicing efficiency is about the same in both tissues (Fig. 4, lanes 5′ and 6′). Controls for contaminating genomic DNA show little amplification (Fig. 4, lanes 7, 8, 11, 12, 7′, and 8′), indicating that the 599-bp bands are from the unspliced pre-mRNA.

DISCUSSION

In the CNS, all four *Ddc* exons (ABCD) are included in the mRNA, whereas in the hypoderm, exon B is skipped to generate a three-exon mRNA (ACD) (Fig. 5). Our previous data show that the splicing specificity of the heat shock-induced *Hsp70/Ddc* transcripts is affected during heat shock, leading to the inappropriate accumulation of the CNS splice form in the hypoderm (32). The splicing specificity of endogenous *Ddc* transcripts is similarly affected, even in the absence of the abundant *Ddc* transcripts produced from the *Hsp70/Ddc* transgene during heat shock. These results suggest that the hypodermal splicing pathway is actively regulated and that the shift in splicing specificity is due to heat shock rather than a titration of splicing factors on the abundantly expressed *Hsp70/Ddc* RNAs (32). In this report, we show that deletion of *Ddc* intron ab sequences disrupts the hypodermal splicing specificity, whereas the CNS splicing specificity is unaffected. That loss

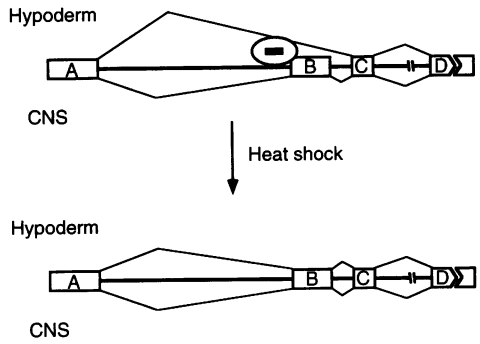

FIG. 5. Blockage model for the regulation of *Ddc* alternative splicing. Splicing to exon B is blocked by a negative regulatory factor shown as an ellipse with a bar in the center. Heat shock relieves this negative regulatory mechanism and allows splicing to exon B in the hypoderm.

of *cis* sequences selectively affects the hypodermal splicing reinforces our previous model that the hypodermal splicing pathway is actively regulated.

The regulated exclusion of exon B in the hypoderm could be achieved by either a negative mechanism blocking splicing to exon B or a positive mechanism activating the exon C 3′ splice site, such that it is used preferentially to the exon B 3′ splice site. In this report, we distinguish between these two general classes of models by localizing the *cis*-regulatory sequences responsible for *Ddc* alternative splicing. By examining transcripts from a fusion gene, *Hsp70/ftz1.DdcB*(l), which contains a heterologous *ftz* 5′ splice site joined to *Ddc* intron ab and exon B under the control of the basally expressed *Hsp70* promoter, we show that *Ddc* intron ab and exon B are sufficient to prevent splicing to exon B in the hypoderm. The *Hsp70/ftz1.DdcB*(l) primary transcript is not spliced in the hypoderm, such that the unspliced pre-mRNA accumulates, whereas the primary transcript is spliced efficiently in the CNS. This result shows that the hypoderm-specific inhibition of splicing can occur in the absence of competition from the exon C 3′ splice site, indicating that the exon C 3′ splice site is not required for this regulation. Heat shock relieves the blockage of *Hsp70/ftz1.DdcB*(l) splicing in the hypoderm, leading to the accumulation of the spliced products in the hypoderm. This is consistent with the effects of heat shock on *Ddc* alternative splicing, in which splicing to exon B occurs in the hypoderm during heat shock (32). These results indicate that heat shock affects *Ddc* alternative splicing and the splicing of this two-exon fusion gene in a similar fashion, showing that the effect of heat shock on *Ddc* alternative splicing is due to a relief of an inhibitory mechanism rather than to a change in splicing specificity. These data strongly support the notion that *Ddc* alternative splicing is regulated by a blockage mechanism preventing splicing to exon B in the hypoderm and that heat shock abolishes this inhibitory mechanism (Fig. 5).

We wish to emphasize that this is the simplest model that explains our results. One can envisage more complex, multicomponent regulatory mechanisms that cannot be ruled out by our current data. As an example, splicing to *Ddc* exon B could be inhibited by an RNA secondary structure within intron ab, such that splicing to exon B is normally inefficient. In the CNS, an activating factor that is heat shock stable could facilitate splicing to exon B. Heat shock or deletion of intron ab sequences could relieve this inhibitory RNA secondary structure, leading to inclusion of exon B even in the hypoderm where the activator is absent. We think that this specific model is unlikely, since heat shock can shift the hypodermal splicing toward the CNS splicing profile at temperatures as low as 30°C (32). Furthermore, the *Hsp70/ftz1.DdcB*(s) and *Hsp70/ftz1.DdcBC*(s) genes must by this model delete this secondary structure but retain the site for the putative CNS activator. Clearly, more detailed molecular and biochemical studies will be required to discern the precise mechanisms of this regulation.

This study provides another example of negative splicing regulation in *D. melanogaster*, in addition to the previously characterized *Sxl* (14), *tra* (35), *suppressor of white apricot* (4, 42), and P-element transposase (21, 34) genes. The negative regulatory mechanism controlling *Ddc* alternative splicing differs from these examples in that it controls a neural versus nonneural splicing choice. It is quite surprising that the *Ddc* CNS-specific exon appears to be included by default, since inclusion of mammalian neural-specific exons is often regulated in neural tissues (5, 6, 36).

The blockage mechanism proposed for *Ddc* alternative splicing is most similar to that controlling *tra* alternative splicing. The alternative splicing of *tra* involves a common 5′ splice site and two alternative 3′ splice sites. The upstream non-sex-specific 3′ splice site is used in both sexes, whereas the downstream female-specific 3′ splice site located within the non-sex-specific exon is used only in females (7). Regulation of *tra* female-specific splicing employs a blockage mechanism which inhibits splicing to the non-sex-specific 3′ splice site (35). This blockage is not as complete as that controlling *Ddc* exon B skipping, since splicing to the *tra* non-sex-specific 3′ splice site still occurs in females such that about one-third of *tra* mRNAs are the non-sex-specific splice form (7), whereas splicing to *Ddc* exon B is completely prevented in the hypoderm. Similar to *Ddc*, the 5′ portion of the *tra* non-sex-specific exon and its upstream intron are sufficient to block splicing to the non-sex-specific 3′ splice site (35). Point mutations in the polypyrimidine tract of the *tra* non-sex-specific 3′ splice site substantially reduce the use of the female-specific 3′ splice site, indicating that these mutations relieve inhibition of splicing to the non-sex-specific 3′ splice site (35). This observation suggests that the polypyrimidine tract is the target *cis* sequence for *Sxl* regulation of *tra* alternative splicing (35). In vitro binding assays have shown that the *Sxl* protein has a higher binding affinity to this polypyrimidine tract than the essential splicing factor U2AF, which is necessary for the binding of U2 small nuclear ribonucleoprotein to the branch point site (41). Mutations in this polypyrimidine tract also abolish *Sxl* binding in vitro (17, 41). These results suggest that *Sxl* prevents splicing to the non-sex-specific 3′ splice site by blocking U2AF binding to the polypyrimidine tract. Whether the regulation of *Ddc* alternative splicing employs a similar regulatory mechanism remains to be determined.

By analyzing splicing of two other fusion genes, *Hsp70/ftz1.DdcB*(s) and *Hsp70/ftz1.DdcBC*(s), which retain only 84 bp of *Ddc* intron ab, we show that there are most likely multiple *cis*-regulatory sequences within intron ab. Splicing of transcripts from these genes shows reduced tissue specificity of the regulated splicing relative to the comparable genes, *Hsp70/ftz1.DdcB*(l) and *Hsp70/ftz1.DdcBC*(l), which contain 528 bp of intron ab.

Regulation of *Sxl* alternative splicing also requires multiple *cis* elements (15). *Sxl* alternative splicing involves inclusion of the male-specific exon in males and exclusion of this exon in females. Female-specific splicing is negatively regulated by preventing splicing to the male exon, which is used by default in males. Splicing to the *Sxl* male exon is completely blocked in females, and the regulatory mechanism preventing the use of

the *Sxl* male 3′ splice site is complex. Intron sequences both upstream and downstream of the male exon are involved in this regulation (15).

The identity of the *trans*-acting repressor(s) that interacts with the *Ddc cis*-regulatory sequences remains to be determined. The *cis* sequences could be required either for the binding of multiple factors or for the high-affinity binding of a single regulator to an extended binding site. Heat shock abolishes this blockage mechanism by either inactivating the heat-labile negative regulator(s) or activating a heat shock-inducible factor(s) which can relieve specific binding of the negative regulator(s) to the *cis*-regulatory regions. Combining the powerful genetic approaches feasible in *D. melanogaster* and in vitro biochemical studies may elucidate the identity of this repressor(s) and the mechanism by which the function of this repressor(s) is inactivated by heat shock.

ACKNOWLEDGMENTS

We thank Paul Adler, Nancy Lewis, and Serge Birman for helpful discussions throughout the course of this work and for critical comments on the manuscript.

This work was supported by NIH grant GM-27318 to J.H. J.S. was supported by an NIH Developmental Biology predoctoral training grant.

REFERENCES

1. **Beall, C., and J. Hirsh.** 1987. Regulation of the *Drosophila* dopa decarboxylase gene in neuronal and glial cells. Genes Dev. **1:**510–520.
2. **Bell, L., J. Horabin, P. Schedl, and T. Cline.** 1991. Positive autoregulation of *Sex-lethal* by alternative splicing maintains the female determined state of *Drosophila*. Cell **65:**229–239.
3. **Bell, L., E. Maine, P. Schedl, and T. Cline.** 1988. *Sex-lethal*, a *Drosophila* sex determination switch gene, exhibits sex-specific RNA splicing and sequence similarity to RNA binding proteins. Cell **55:**1037–1046.
4. **Bingham, P. M., T. B. Chou, I. Mims, and Z. Zachar.** 1988. On/off regulation of gene expression at the level of splicing. Trends Genet. **4:**134–138.
5. **Black, D.** 1991. Does steric interference between splice sites block the splicing of a short c-src neuron-specific exon in non-neuronal cells? Genes Dev. **5:**389–402.
6. **Black, D. L.** 1992. Activation of c-src neuron-specific splicing by an unusual RNA element *in vivo* and *in vitro*. Cell **69:**795–807.
7. **Boggs, R., P. Gregor, S. Idriss, J. Belote, and J. McKeown.** 1987. Regulation of sexual differentiation in *D. melanogaster* via alternative splicing of RNA from the *transformer* gene. Cell **50:**739–747.
8. **Bray, S. J., W. A. Johnson, J. Hirsh, U. Heberlein, and R. Tjian.** 1988. A cis-acting element and associated binding factor required for CNS expression of the *D. melanogaster dopa decarboxylase* gene. EMBO J. **7:**177–188.
9. **Burtis, K., and B. Baker.** 1989. *Drosophila doublesex* gene controls somatic sexual differentiation by producing alternatively spliced mRNAs encoding related sex-specific polypeptides. Cell **56:**997–1010.
10. **Chomczynski, P., and N. Sacchi.** 1987. Single-step method of RNA isolation by acid guanidinium thiocyanate-phenol-chloroform extraction. Anal. Biochem. **162:**156–159.
11. **Emeson, R. B., F. Hedjran, J. M. Yeakley, J. W. Guise, and M. G. Rosenfeld.** 1989. Alternative production of calcitonin and CGRP mRNA is regulated at the calcitonin-specific splice acceptor. Nature (London) **341:**76–80.
12. **Green, M. R.** 1991. Biochemical mechanisms of constitutive and regulated pre-mRNA splicing. Annu. Rev. Cell Biol. **7:**559–599.
13. **Hedley, M., and T. Maniatis.** 1991. Sex-specific splicing and polyadenylation of *dsx* pre-mRNA requires a sequence that binds specifically to *tra*-2 protein *in vitro*. Cell **65:**579–586.
14. **Horabin, J. I., and P. Schedl.** 1993. Regulated splicing of the *Drosophila Sex-lethal* male exon involves a blockage mechanism. Mol. Cell. Biol. **13:**1408–1414.
15. **Horabin, J. I., and P. Schedl.** 1993. *Sex-lethal* autoregulation requires multiple *cis*-acting elements upstream and downstream of the male exon and appears to depend largely on controlling the use of the male exon 5′ splice site. Mol. Cell. Biol. **13:**7734–7746.
16. **Hortsch, M., A. Bieber, N. H. Patel, and C. S. Goodman.** 1990. Differential splicing generates a nervous-system specific form of *Drosophila* neuroglian. Neuron **4:**697–709.
17. **Inoue, K., K. Hoshijima, H. Sakamoto, and Y. Shimura.** 1990. Binding of the *Drosophila Sex-lethal* gene product to the alternative splice site of *transformer* primary transcript. Nature (London) **344:**461–463.
18. **Karess, R. E., and G. M. Rubin.** 1984. Analysis of P transposable element functions in *Drosophila*. Cell **38:**135–146.
19. **Konrad, K. D., and J. L. Marsh.** 1987. Developmental expression and spatial distribution of dopa decarboxylase in *Drosophila*. Dev. Biol. **122:**172–185.
20. **Kornfeld, K., R. B. Saint, P. A. Beachy, P. J. Harte, D. A. Peattie, and D. S. Hogness.** 1989. Structure and expression of a family of *Ultrabithorax* mRNAs generated by alternative splicing and polyadenylation in *Drosophila*. Genes Dev. **3:**243–258.
21. **Laski, F. A., and G. M. Rubin.** 1989. Analysis of the cis-acting requirements for germ-line-specific splicing of the P-element ORF2-ORF3 intron. Genes Dev. **3:**720–728.
22. **Maniatis, T.** 1991. Mechanisms of alternative pre-mRNA splicing. Science **251:**33–34.
23. **Martinez, R., B. Mathey-Prevot, A. Bernards, and D. Baltimore.** 1987. Neuronal $pp60^{c\text{-}src}$ contains a six-amino acid insertion relative to its non-neuronal counterpart. Science **237:**411–415.
24. **McKeown, M.** 1992. Alternative mRNA splicing. Annu. Rev. Cell Biol. **8:**133–155.
25. **Morgan, B., W. A. Johnson, and J. Hirsh.** 1986. Regulated splicing produces different forms of dopa decarboxylase in the central nervous system and hypoderm of *Drosophila melanogaster*. EMBO J. **5:**3335–3342.
26. **Pirrotta, V.** 1988. Vectors for P-mediated transformation in *Drosophila*, p. 437–456. *In* R. L. Rodriguez and D. T. Denhardt (ed.), Vectors, a survey of molecular cloning vectors and their uses. Butterworths, Boston.
27. **Pyper, J. M., and J. B. Bolen.** 1990. Identification of a novel neuronal c-*src* exon expressed in human brain. Mol. Cell. Biol. **10:**2035–2040.
28. **Rio, D. C.** 1993. Splicing of pre-mRNA: mechanism, regulation and role in development. Curr. Opin. Genet. Dev. **3:**574–584.
29. **Rosenfeld, M. G., S. G. Amara, and R. M. Evans.** 1984. Alternative RNA processing: determining neuronal phenotype. Science **225:**1315–1320.
30. **Ryner, L. C., and B. S. Baker.** 1991. Regulation of *doublesex* pre-mRNA processing occurs by 3′-splice site activation. Genes Dev. **5:**2071–2085.
31. **Santoni, M. J., D. Barthels, G. Vopper, A. Boned, C. Goridis, and W. Wille.** 1989. Differential exon usage involving an unusual splicing mechanism generates at least eight types of NCAM cDNA in mouse brain. EMBO J. **8:**385–392.
32. **Shen, J., C. J. Beall, and J. Hirsh.** 1993. Tissue-specific alternative splicing of the *Drosophila dopa decarboxylase* gene is affected by heat shock. Mol. Cell. Biol. **13:**4549–4555.
33. **Siebel, C. W., L. D. Fresco, and D. C. Rio.** 1992. The mechanism of somatic inhibition of *Drosophila* P-element pre-mRNA splicing: multiprotein complexes at an exon pseudo-5′ splice site control U1 snRNP binding. Genes Dev. **6:**1386–1401.
34. **Siebel, C. W., and D. C. Rio.** 1990. Regulated splicing of the Drosophila P transposable element third intron in vitro: somatic repression. Science **248:**1200–1208.
35. **Sosnowski, B., J. Belote, and M. McKeown.** 1989. Sex-specific alternative splicing of RNA from the *transformer* gene results from sequence-dependent splice site blockage. Cell **58:**449–459.
36. **Stamm, S., M. Q. Zhang, T. G. Marr, and D. M. Helfman.** 1994. A sequence compilation of comparison of exons that are alternatively spliced in neurons. Nucleic Acids Res. **22:**1515–1526.
37. **Stroeher, V. L., C. Gaiser, and R. L. Garber.** 1988. Alternative RNA splicing that is spatially regulated: generation of transcripts

from the *Antennapedia* gene of *Drosophila melanogaster* with different protein-coding regions. Mol. Cell. Biol. **8:**4143–4154.
38. **Tacke, R., and C. Goridis.** 1991. Alternative splicing in the neural cell adhesion molecule pre-mRNA: regulation of exon 18 skipping depends upon the 5′ splice site. Genes Dev. **5:**1416–1429.
39. **Tian, M., and T. Maniatis.** 1992. Positive control of pre-mRNA splicing. Science **256:**237–240.
40. **Tian, M., and T. Maniatis.** 1993. A splicing enhancer complex controls alternative splicing of *doublesex* pre-mRNA. Cell **74:**105–114.
41. **Valcarcel, J., R. Singh, P. D. Zamore, and M. R. Green.** 1993. The protein *Sex-lethal* antagonizes the splicing factor U2AF to regulate alternative splicing of *transformer* pre-mRNA. Nature (London) **362:**171–175.
42. **Zachar, Z., T. B. Chou, and P. M. Bingham.** 1987. Evidence that a regulatory gene autoregulates splicing of its transcript. EMBO J. **6:**4105–4111.